nature energy

REVIEW ARTICLE

https://doi.org/10.1038/s41560-019-0405-3

Challenges and opportunities towards fast-charging battery materials

Yayuan Liu[1], Yangying Zhu[1] and Yi Cui[1,2*]

Extreme fast charging, with a goal of 15 minutes recharge time, is poised to accelerate mass market adoption of electric vehicles, curb greenhouse gas emissions and, in turn, provide nations with greater energy security. However, the realization of such a goal requires research and development across multiple levels, with battery technology being a key technical barrier. The present-day high-energy lithium-ion batteries with graphite anodes and transition metal oxide cathodes in liquid electrolytes are unable to achieve the fast-charging goal without negatively affecting electrochemical performance and safety. Here we discuss the challenges and future research directions towards fast charging at the level of battery materials from mass transport, charge transfer and thermal management perspectives. Moreover, we highlight advanced characterization techniques to fundamentally understand the failure mechanisms of batteries during fast charging, which in turn would inform more rational battery designs.

Compared with internal combustion engine vehicles, the limited driving range and long charging time of electric and plug-in hybrid vehicles (EVs and PHEVs) cause 'range anxiety' among existing owners while posing barriers to market adoption by potential new owners. Current EVs and PHEVs rely primarily on residential and workplace charging (levels 1 and 2, respectively) with recharge time on the order of tens of hours (Fig. 1a)[1]. The Society of Automotive Engineers in the United States defines (standard J1772) level 1 charging as 120 V alternating current (a.c.) with a maximum charging power of 1.9 kW (16 A maximum current), and level 2 charging as 208 to 240 V a.c. with a maximum charging power of 19.2 kW (80 A maximum current)[2]. Burgeoning direct current (d.c.) charging stations with a maximum power of approximately 50 kW deployed to date can extend the flexibility of EVs by adding 60–80 miles of driving range per 20 minutes of charging (J1772 defines d.c. charging as 200–450 V with current up to 80 A and 200 A for d.c. levels 1 and 2, respectively)[2]. Superchargers exclusive to Tesla vehicles offer the fastest recharge rate of 120 kW (480 V d.c., these chargers can technically support up to 145 kW charging), shortening the refuelling time for 200 miles down to approximately 30 minutes. Nevertheless, the state-of-the-art charging capabilities are still far from offering consumers the same refuelling experience as conventional vehicles. As a result, the US Department of Energy has identified extreme fast charging (XFC) as a critical challenge to ensure mass adoption of EVs and PHEVs, curb greenhouse gas emissions and, in turn, provide nations with greater energy security[3].

The US Advanced Battery Consortium goals for low-cost/fast-charge EV batteries by 2023 is 15 minutes charging for 80% of the pack capacity, along with other key metrics (US$75 kWh^{-1}, 550 Wh l^{-1} and 275 Wh kg^{-1} at the cell level). Figure 1b shows a theoretical plot of recharge time and the corresponding charging rate as a function of charging power[4]. At a specific power, a larger battery pack requires a longer charging time. Therefore, chargers should be scaled based on the pack size. If the pack size is large (for example, >90 kWh), a charging power of at least 300 kW is needed to meet the 15-minute recharge goal. Bigger packs, however, will offer longer driving range for the same state of charge (SoC) increment.

The successful realization of XFC requires extensive research and development across multiple levels, spanning from charging infrastructure to vehicle designs and down to individual batteries[4–7]. Prominent challenges include balancing the load on the electric grid during unscheduled XFC events[7], developing viable business models for the implementation of charging stations[7], upgrading vehicles' electronic and thermal management systems with minimal cost[5,6] and so on. In all cases, lithium (Li)-ion battery technologies present a major technical barrier to fast charging[4]. The current high-energy cells with graphite anodes and metal oxide cathodes in liquid electrolytes are unable to achieve the XFC goal without adversely impacting battery performance and safety. When batteries are charged at high rates, various polarizations (ohmic, concentration and electrochemical) inside the battery will result in limited utilization of active materials, increased propensity for Li plating, excessive heat generation and so on[8].

To help effectively address these challenges, this Review surveys the main limitations of current battery materials towards XFC from mass transport and charge transfer perspectives. Battery thermal challenges under fast-charging conditions are also discussed. Moreover, as increased charging rates will probably introduce new degradation mechanisms, this Review also highlights advanced characterization techniques that can deepen our fundamental understanding of the impacts of XFC and inform more rational material designs.

Challenges for electrolyte mass transport

The electrolyte transport properties play a decisive role in determining how fast a cell can be charged. The ohmic voltage drop across the electrolyte, particularly at low temperatures, can result in limited deployable capacity due to an early hitting of the cut-off voltage[9]. More importantly, the non-unity Li^+ transference number (t^+, defined as the fraction of ionic current contributed by Li^+ movement) of liquid electrolytes will inevitably establish a concentration gradient during battery operation, which becomes more pronounced at higher currents (Fig. 2a)[10,11]. Under sustained fast charging, Li ions can be depleted at a certain depth within the

[1]Department of Materials Science and Engineering, Stanford University, Stanford, CA, USA. [2]Stanford Institute for Materials and Energy Sciences, SLAC National Accelerator Laboratory, Menlo Park, CA, USA. *e-mail: yicui@stanford.edu

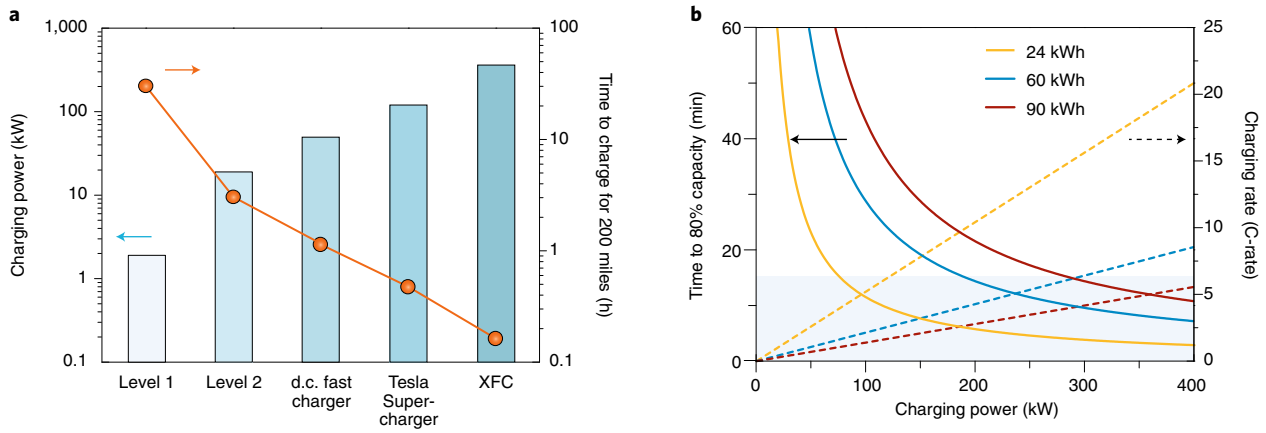

Fig. 1 | Overview of the technical requirements for EV battery fast charging. a, Comparison of currently available charging methods with XFC. Levels 1 and 2 are based on the maximum charging power defined by The Society of Automotive Engineers standard J1772 and d.c. fast charger is based on a maximum power of approximately 50 kW deployed to date[1,2]. Tesla Supercharger is based on the current 120 kW maximum rate of Supercharging V2 stations[1]. XFC with a charging power of 350 kW is used for calculation. The vehicle energy consumption is assumed to be 285 Wh per mile and charging efficiency is not considered[4]. **b**, Theoretical plot of recharge time up to 80% capacity (solid lines) and the corresponding charging rate (dashed lines) as a function of charging power for three battery pack sizes. The shaded area corresponds to charging powers that meet the US Advanced Battery Consortium goals for low-cost/fast-charge EV batteries (15 minutes charging for 80% of the pack capacity).

anode, beyond which the active materials can no longer be utilized. At a certain C-rate, the concentration polarization increases appreciably with electrode thickness due to increased current density; therefore, low-areal-capacity electrodes are preferred for XFC purposes[11]. Unfortunately, this is contradictory to the current design principles of EV batteries, where increasing active material loading is a primary means to improve pack-level energy density for extended driving range, while simultaneously lowering the cost. To resolve this dilemma, major research thrusts have focused on engineering electrolytes and improving electrode architectures.

Improving the electrolyte ionic conductivity. Pioneering work has improved the low-temperature ionic conductivity of carbonate-based electrolytes with aliphatic ester co-solvents, which have low viscosity and freezing point[12,13]. In one case, the addition of 20 wt% methyl acetate led to an approximately 50% increase in ionic conductivity compared with baseline electrolyte, and the corresponding $Li[Ni_{0.5}Mn_{0.3}Co_{0.2}]O_2$ (NMC532)/graphite cells showed improved cycling performance up to 2C (ref. [12]). Nonetheless, short-chain esters typically show inferior oxidation stability than baseline electrolytes and the resulting solid electrolyte interphase (SEI) is less favourable[14]. Therefore, judicious selection of additional film-forming additives is needed for ester-rich electrolytes. Given the excessive heat generated during XFC, the relatively low boiling point of the studied esters may be a concern, which requires further investigation. Moreover, large local variations in salt concentrations can be expected at high charging rates; therefore, versatile electrolyte formulations are desired to maintain a high ionic conductivity across a wide concentration window.

While significant improvement in the ionic conductivity of liquid electrolytes may be difficult, engineering separators seems more attainable to enhance the overall ion transport, as standard separators often reduce the electrolyte ionic conductivity in the pore space by an order of magnitude[15]. Inquiring minds may refer to a recent review for a comprehensive survey of various separator chemistries and surface modifications[16].

Improving the electrolyte Li^+ transference number. The classical Newman model emphasized the importance of transference number, showing that a near unity t^+ can offer significantly improved rate performance over systems with $t^+ \sim 0.2$ due to alleviated concentration overpotential, even if the conductivity is decreased by an order of magnitude[10]. Figure 2b shows the attainable SoC before reaching the cut-off voltage as a function of charge rate for cells with different t^+. Although little difference is observed at low current densities, the advantages of high t^+ can be clearly observed at rates above 2C (ref. [17]). However, current liquid electrolytes usually have t^+ below 0.5, due to the bulky solvation sheath around Li^+ compared with that of typical anions[18]. Therefore, for near-term applications, it is critical to improve the t^+ of the existing liquid electrolytes. One approach to achieve this goal is to use Li salts with bulky anions[19,20]. In an early demonstration with lithium bis(perfluoropinacolato)borate (giant anion with 24 fluorine atoms), the Li^+ diffusivity was measured to be greater than that of the anion[19]. Further along this line, anions were shown to be tethered together to create Li-neutralized polyanions dissolved in polar aprotic solvents (Fig. 2c)[21]. Using a model short-chain polyether with pendent lithium sulfonate moieties, the obtained polyelectrolyte solutions exhibited a maximum t^+ of 0.98 and ionic conductivity on the order of 1 mS cm^{-1}. Nevertheless, a strong Lewis basic solvent (dimethyl sulfoxide) was needed to maximize the solubility and dissociation of the ionic species. Therefore, opportunities exist to tune the backbone and anion chemistry of polyelectrolytes to be compatible with battery-relevant solvents. Other examples include anchoring anions on nanoparticles[22] and utilizing the emerging concept of 'solvent-in-salt', where a high t^+ value of 0.73 was achieved with concentrated ether-based electrolytes due to an incomplete Li^+ solvation[23]. As the viscosity of electrolytes increases appreciably with polymer/salt concentration, an exquisite balance needs to be struck between conductivity, transference number and viscosity in these systems. Nevertheless, improving the t^+ of liquid electrolytes represents an important yet under-researched approach, and readers are referred to a more exhaustive review on this topic[17].

Solid electrolytes have potential benefits in energy density, operable temperature range, dendrite resistance and safety compared with liquid counterparts[24]. Inorganic solid electrolytes have unity t^+ to eliminate concentration gradient, and some possess high ionic conductivity on par with liquids[25]. Unfortunately, they are limited by their brittle nature when configured in a thin form factor and high interfacial impedance, which usually requires special structural

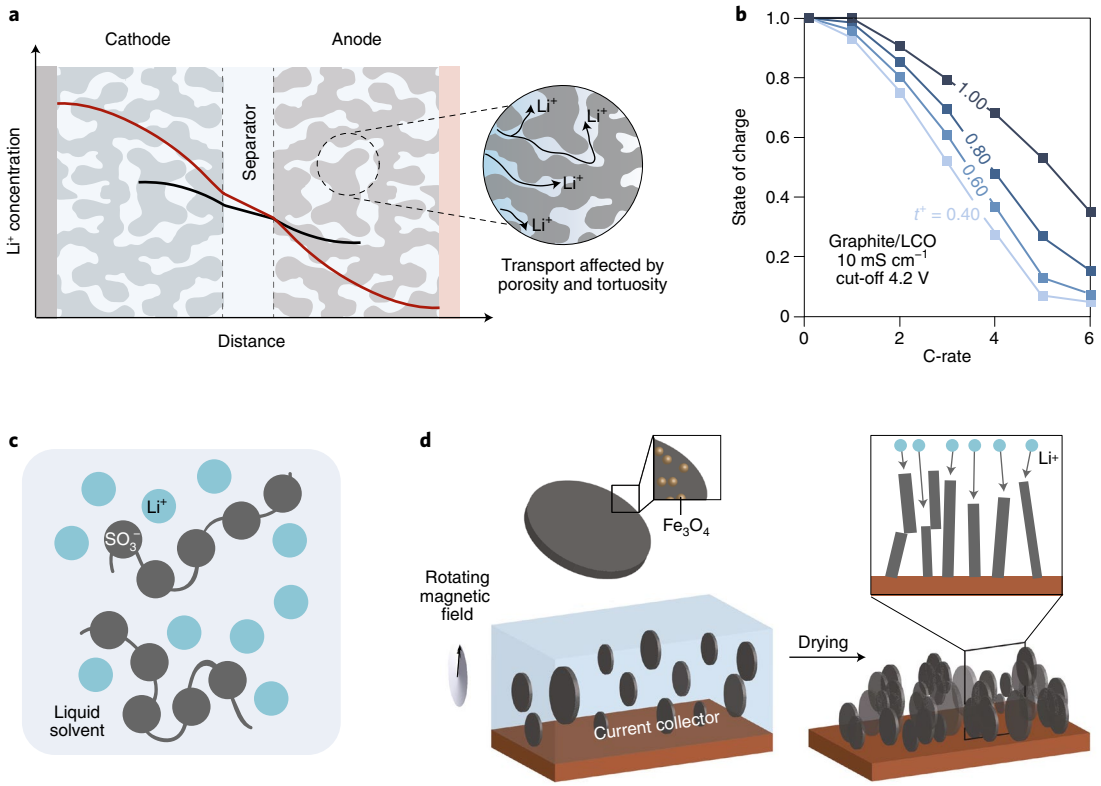

Fig. 2 | Electrolyte mass transport limitations during fast charging and possible mitigation strategies. a, Schematic of the electrolyte mass transport limitations during XFC. Slow diffusion of Li^+ through the electrolyte and the porous electrodes as well as the non-unity Li^+ transference number can result in significant ohmic and concentration polarization, leading to incomplete utilization of active materials. The black and red curves schematically illustrate the spatial distribution of Li^+ concentration in the case of thin and thick electrodes, respectively. Concentration polarization is more pronounced for thick electrodes and electrodes with low porosity and/or high tortuosity. **b**, Finite element analysis of attainable SoC versus charge rate for electrolyte with an ionic conductivity of 10 mS cm^{-1} and variable t^+ (ref. [17]). The model was based on graphite anode (thickness = 91.8 μm, porosity = 0.25), LCO cathode (thickness = 100 μm, porosity = 0.20) and a separator in between (thickness = 25 μm, porosity = 0.39). Detailed information on the modelling can be found in ref. [17]. **c**, The Li^+ transference number of liquid electrolytes can be improved using Li-neutralized polyanions dissolved in polar aprotic solvents. For example, poly(allyl glycidyl ether-lithium sulfonate) (short-chain polyethers with pendent lithium sulfonate moieties) dissolved in dimethyl sulfoxide exhibited a maximum t^+ of 0.98 and ionic conductivity on the order of 1 mS cm^{-1} (ref. [21]). **d**, Schematic showing that a low-tortuosity anode can be obtained by aligning graphite flakes decorated with superparamagnetic nanoparticles using a magnetic field during the electrode drying step, and the corresponding schematic depicting the shortened Li^+ diffusion path[34]. Panels adapted from: **b**, ref. [17], American Chemical Society; **c**, ref. [21], American Chemical Society; **d**, ref. [34], Springer Nature Ltd.

design to realize high-current-density cycling[26,27]. In contrast, dry polymer electrolytes exhibit better flexibility and interfacial adhesion. Many polymeric single-ion conductors have been reported by covalently linking anions to the polymer backbone, the progress of which has been well summarized recently[28]. However, the ionic conductivity of these polymer electrolytes at room temperature (<10^{-5} S cm^{-1}) remains at least two orders of magnitude lower than that of standard liquid electrolytes[17,28].

As solid electrolytes have densities considerably higher than liquid electrolytes, they must be fabricated adequately thin for practical devices (<25 μm, at least comparable to the thickness of commercial separators). However, most solid electrolytes are studied as thick films (often >100 μm), and there are limited methods described in open literature to fabricate thin solid electrolytes in a scalable, low-cost manner[26], other than ref. [27]. In this regard, one solution might be composites consisting of single-layer inorganic solid electrolyte particles embedded in a polymeric matrix, which have been shown to achieve high ionic conductivity through the inorganic phase along with decent flexibility and reduced thickness[29]. A porous, robust polymeric scaffold, not necessarily ionically conducting, can also accommodate solid polymer electrolytes to enhance their mechanical strength at reduced thickness. Solvent-swollen ionomer is another promising alternative, where porous anionic polymer membranes are filled with liquid solvents to enhance Li^+ mobility in the liquid phase[30,31]. Though not technically classified as 'solid electrolyte' and some desirable mechanical and safety features might be compromised, solvent-filled ionomers can simultaneously achieve near-unity t^+ and high ionic conductivity.

Reducing the electrode tortuosity. Reducing the ion-path tortuosity is an important direction to accelerate diffusive Li^+ transport in the electrolyte phase across the porous electrode, which is particularly crucial for thick electrodes[32,33]. A recent study successfully aligned graphite flakes coated with superparamagnetic nanoparticles perpendicularly to the current collector by applying a magnetic field during electrode fabrication (Fig. 2d)[34]. The out-of-plane tortuosity of the aligned anode was reduced by a factor of nearly four, allowing it to be cycled at rates up to 2C with a specific capacity three times higher than a randomly oriented electrode. A similar microstructure alignment concept has also been applied to cathodes. For example, lithium cobalt oxide (LCO) electrodes with porous channels preferentially oriented in the transport direction have been fabricated by co-extrusion with sacrificial pore formers[35], directional freezing of aqueous suspensions[36], or magnetic

alignment of sacrificial magnetic microrods or ferrofluid droplets[37]. Nevertheless, the cycling rates demonstrated in these studies cannot meet the requirement for XFC yet, implying significant room for improvement, and more economical methods are to be explored for large-scale fabrication.

The laminated structure of conventional batteries limits the ion transport between electrodes to be only one-dimensional in nature. Correspondingly, the concept of extending battery architecture into three dimensions has been proposed for more than a decade[38]. The ideal electrode structure consists of three-dimensional (3D) interpenetrating electron and ion pathways with short transport distance. Nevertheless, the complexity of fabrication confines the current 3D devices to very small sizes (usually microbatteries) and limited choices of electrode materials[39]. More reliable, large-scale fabrication approaches need to be explored to enable 3D batteries for XFC applications. Another opportunity to facilitate mass transport is to introduce convection inside the battery by, for example, circulating electrolyte through the electrodes. This concept could potentially mitigate the concentration gradient and render diffusion necessary only at the local scale, though it has not been demonstrated and may require a major overhaul of battery architectures. Utilizing electrokinetics phenomena in porous media under an electric field, a recent study applied a 3D cross-linked polyethylenimine sponge to enrich Li^+ concentration on the electrode surface[40].

Light-weighting the battery design. An effective way to resolve the electrode thickness versus rate performance dilemma is by light-weighting the battery, such that thinner electrodes can be employed for XFC without severely compromising the energy density. This idea is straightforward yet largely overlooked by the battery community. For example, a copper current collector accounts for approximately 10% of the total cell weight[41]. Compared with copper (8.96 g cm^{-3}), polymers have much lower densities (~1 g cm^{-3}). Therefore, by replacing the majority of the current collector volume with a robust, ultra-thin polymeric backbone on which a copper thin film is deposited, appreciable parasitic weight reduction can be achieved.

Challenges for electrode charge transfer

Li plating on graphite is a main culprit of fast-charging problems and occurs when the charging rate exceeds the intercalation rate into the graphite crystal structure. The charge-transfer overpotential, along with ohmic and concentration polarizations, drive the anode potential below the Li^+/Li^0 equilibrium potential. Metallic Li can cause electrolyte decomposition, Li inventory loss and internal micro-shorts[4]. In the best scenario, plated Li can be removed through a very slow discharge process. However, it is not necessarily feasible as the discharge of EV batteries is dictated by users and traffic conditions, and not all Li deposits are electrically connected to the anode[11].

Charge transfer at the graphite anode, defined as the process during which Li ions meet electrons, can be divided into the following steps (Fig. 3a): Li^+ desolvation at the SEI/electrolyte interface; diffusion of naked Li^+ through the SEI; electron reception at the anode/SEI interface and solid-state Li diffusion in carbon galleries[42]. While it is still debatable whether Li desolvation or diffusion is the limiting step[43–45], all three steps are important in controlling the rate performance and will be discussed individually.

Accelerating Li^+ desolvation. A large body of literature argues that Li^+ desolvation dictates the charge-transfer kinetics[43,44]. Given its small ionic radius, Li^+ exerts strong Coulombic attractions towards solvent molecules, hindering the desolvation process (activation energy 50–60 kJ mol^{-1}). The desolvation energy of Li^+ has been shown to be halved in ionic liquids, probably due to the disruption of the tight solvation sheath in the presence of large organic cations[41]. The desolvation kinetics of different electrolyte systems remains largely unexplored, which can be evaluated by, for example, measuring the exchange current of the Li^+/Li^0 couple using a microelectrode[46]. We suggest the introduction of charge-delocalized species in the form of electrolyte additive, or more effectively, anode surface coating, to reduce the energy barrier for Li^+ desolvation. For example, polymeric binders with carboxylic acid functional groups have been shown to participate in the competitive solvation of Li^+ at the graphite surface, assisting Li^+ dissociation from solvent molecules[47]; special anions may also weaken the Li^+–solvent interaction[48].

Low-resistance SEI. Electrolyte additives have always been a centrepiece in tuning SEI properties, as thoroughly discussed in classical reviews[18,49]. An ideal SEI for XFC should be thin, compact and rich in ionically conductive domains. For more rational selection of additives, it is important to correlate the physiochemical properties of the SEI with its ionic conductivity. The emerging cryogenic electron microscopy (cryo-EM), capable of interrogating pristine SEI at the nano- and atomic scales, can be a powerful complement to the conventional electrochemical and surface-sensitive characterizations for such studies[50–52].

An alternative to promote Li^+ transport through the SEI is to precondition the graphite surface with an artificial SEI. In one example, a liquid polyether (polyethylene glycol *tert*-octylphenyl ether, PEGPE) was blended with polyallyl amine to form a multifunctional coating, where the solid-state complexation of Li^+ by PEGPE provided more transport pathways, and its aromatic ring enabled π–π interaction with graphite for strong adhesion, substantially enhancing the charging capacity[53]. In another example, the rate capability of graphite can be improved by an amorphous carbon coating, the isotropic nature of which allows 3D Li^+ transport[54].

Increasing density of active sites. Graphite, being a layered material, shows highly anisotropic solid-state Li diffusivity (D). Though diffusion is reported to be relatively fast parallel to the carbon layers, the rate can be four to five orders of magnitude slower across the basal planes, limiting the overall intercalation kinetics[55]. As the characteristic time (τ) for diffusion is proportional to the square of diffusion length (L, $\tau = L^2/D$), shortening L by increasing the accessible reaction sites can be favourable for XFC.

As Li ions intercalate from the edges of graphite layers, the example of magnetic-field-aligned graphite flakes described earlier to reduce electrode tortuosity can also provide Li ions with easier access to graphite edges[34]. In another study, a multichannel structure was proposed to increase intercalation sites by etching holes on the graphite surface with KOH[56]. Recently, a hybrid anode was fabricated for fast charging by coating amorphous silicon (a-Si) on edge-plane activated graphite (SEAG; Fig. 3b)[57]. The activated edges doubled the reactive surface area, while the a-Si coating increased the energy density and allowed for fast Li^+ transport. The high-areal-capacity SEAG electrode (3.5 mAh cm^{-2}) exhibited an exceptional initial Coulombic efficiency (93.8%) and retained >20% capacity when lithiated galvanostatically at 3C (Fig. 3c). Moreover, the SEAG/LCO full cell (3.4 mAh cm^{-2}) demonstrated no trace of Li plating after 50 cycles under a harsh charging current (7.7 mA cm^{-2}; Fig. 3d). For all these chemical modifications, it is important to activate graphite without significantly increasing the surface area, which can otherwise compromise the Coulombic efficiency. Finally, as the structure, particle size and morphology of graphite significantly impact its charge acceptance, attention needs to be given to evaluating different graphite materials.

Dendrite suppression and early detection. Apart from facilitating the three steps of charge transfer to prevent Li plating during XFC, it is also necessary to incorporate additional measures to ensure battery safety in the event of dendrite formation. Inspirations can be

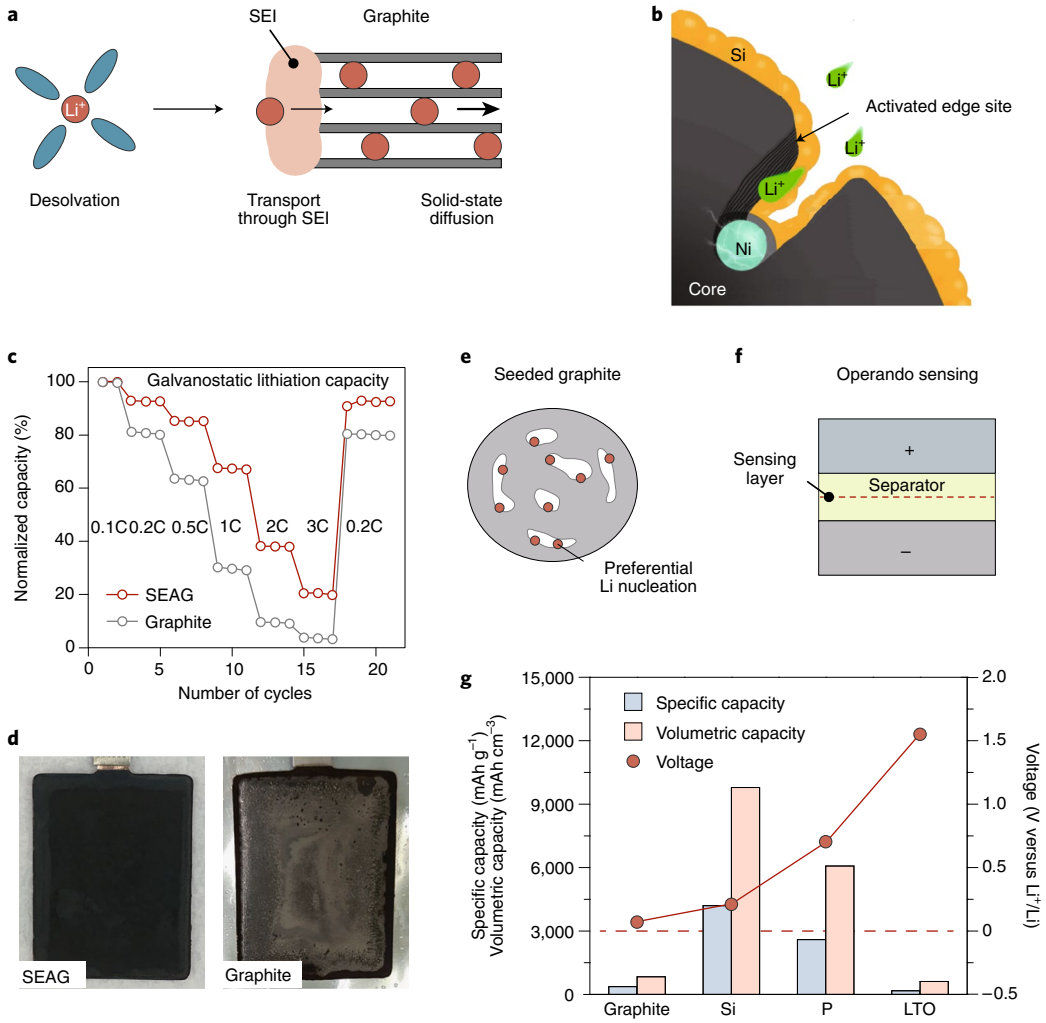

Fig. 3 | Electrode charge-transfer limitations during fast charging and some possible mitigation strategies. a, Schematic showing the three steps of charge transfer at a graphite anode. **b**, Schematic showing the detailed structural characteristics of SEAG. To synthesize the structure, nickel nanoparticles were deposited on mesocarbon microbeads, which were then calcined in a hydrogen atmosphere to activate the graphite edges via catalytic hydrogenation. Subsequently, a graphitic carbon shell and an a-Si nanolayer were homogeneously coated on the graphite particles via consecutive chemical vapour deposition[57]. **c**, Galvanostatic charging capacities of SEAG and graphite at different rates[57]. **d**, Photographs of SEAG and graphite electrode after 50 cycles at 7.7 mA cm^{-2} (ref. [57]). **e**, The adverse effects of Li plating can be alleviated by directing the plating events into the porous space of graphite particles rather than on the outer surface of the electrode. This can be achieved, for example, by seeding graphite with nanoparticles for preferential metallic Li nucleation. **f**, Early detection of Li plating is of paramount importance for battery safety, which can be realized with sensing layers incorporated into battery separators. **g**, The specific capacity, volumetric capacity and lithiation potential of some alternative anode materials[67]. Panels **b**–**d** adapted from ref. [57], Springer Nature Ltd.

drawn from the revitalization of Li-metal-anode research in recent years, where dendrite suppression and early detection is a major research theme[58]. It has been shown that the Li-plating overpotential is substrate dependent with little nucleation barrier on metals with a definite Li solubility (for example, Au, Ag and Zn)[59]. On this basis, a seeded anode design can be envisioned, where nanoparticles favourable for Li nucleation are embedded inside the porous space of graphite particles (Fig. 3e). As a result, if Li plating were to occur, it could be confined inside the anode with reduced risk of reacting with electrolyte and incurring internal short circuit[60].

For non-destructive detection of Li plating, methods employed so far usually involve specialized instrumentation, such as high-precision coulometry and microcalorimetry, which are more suitable for fundamental studies than real applications[61,62]. However, the battery separator can be a powerful platform to be integrated with versatile operando sensing functionalities (Fig. 3f). Voltage sensing for early failure detection has been demonstrated using separators with a polymer–metal–polymer configuration, where a sudden voltage drop between the anode and the metal layer can be indicative of dendrite penetration into the separator[63]. Other possibilities of 'smart separators' include the introduction of a reference electrode for monitoring the exact anode potential, measuring internal battery temperature, the incorporation of thermally triggered flame retardant[64] and so on.

As the propensity for Li plating becomes higher at higher SoC due to both the lower lithiation potential and the reduced diffusion coefficient at high in-plane Li concentration[65], the conventional constant-current/constant-voltage charging is non-ideal for XFC. Alternative charging protocols, such as step-wise charging with lower rate at high SoC, should be explored to avoid accelerated performance decay and safety concerns. However, complex charging protocols naturally encompass a huge parameter space such that the optimization process can become extremely time consuming. Therefore, enabling rapid screening of charging protocols with

advanced computational modelling and machine learning is worthwhile exploring[66].

Alternative anode materials. The close proximity of the graphite potential to that of Li^+/Li^0 makes the material particularly susceptible to Li plating. Therefore, anode chemistries with safer working voltages are attractive for XFC batteries (Fig. 3g)[67]. To this end, lithium titanium oxide ($Li_4Ti_5O_{12}$, LTO) has been extensively evaluated with sufficient data supporting its reliability when charged at high rates (>10C)[68], and has been already employed in commercial fast-charging batteries (for example, Toshiba SCiB, designed to offer 90% charge capacity in 10 minutes). However, the energy density of the corresponding cells can be severely limited by the low capacity (175 mAh g^{-1}) and high potential (approximately 1.55 V versus Li^+/Li^0) of LTO, which is unsuitable for EVs with long driving ranges. Recently, Toshiba demonstrated carbon-coated niobium titanium oxide ($TiNb_2O_7$, TNO) as an alternative to LTO, which has a theoretical capacity comparable to graphite (388 mAh g^{-1}) operating on the Ti^{4+}/Ti^{3+} and Nb^{5+}/Nb^{3+} redox couples[69,70]. The 49 Ah TNO/NMC622 cells demonstrated fast-charging from 0% to 90% SoC in less than 6 minutes and 86% capacity retention after 7,000 cycles at 1C.

Besides working potential, specific capacity is another crucial parameter to consider. High-capacity anodes can reduce the electrode thickness and the charge carrier transport distance, both of which are highly desirable for fast charging. Silicon offers advantageously high theoretical capacity (4,200 mAh g^{-1} based on the weight of Si) with lithiation voltage slightly above that of graphite. Despite the rapid maturation of Si technology, fast charging of Si electrodes at commercial-level mass loading is not widely described in literature[4,71]. Nevertheless, battery companies have disclosed fast-charging capabilities using Si-dominant anodes. Phosphorous (P) is another promising candidate due to the combined advantages of high capacity (2,595 mAh g^{-1} based on the weight of P) and relatively low yet safe lithiation potential (approximately 0.7 V versus Li^+/Li^0), which therefore deserves more research efforts[72,73]. Besides choosing the right materials, structural design towards high electronic conductivity and space-efficient packing is also essential for achieving XFC capability, the common strategies of which have been summarized elsewhere[74].

Li metal has been garnering great research interest recently as the ultimate anode with the highest theoretical capacity. Despite notable progress, Li metal is still plagued by unsolved fundamental issues, such as low Coulombic efficiency and uncontrolled deposition morphology, which tend to exacerbate at high currents[58]. These challenges require painstaking research on electrode architectures[75], surface protections[40] and electrolyte formulations[76], which preclude the deployment of a Li metal anode for XFC batteries in the near term.

Mass transport versus charge transfer. For future research, it is particularly important to decouple the effects of mass transport and charge transfer at both electrodes[11]. Recently, a study investigated the power performance of graphite and NMC separately with symmetric cells and found that graphite showed much more rapid capacity fade at high rates, making it the limiting electrode[77]. However, the charge-transfer impedance of graphite was measured to be lower than that of NMC, indicating that mass transport might be more critical. Nevertheless, given the numerous electrode materials available and the many parameters (areal loading, porosity, electrolyte and so on), the limiting factor may vary and it thus remains an open topic of research.

Battery thermal considerations during fast charging

Temperature is another critical barrier to XFC besides electrolyte ion transport and electrode charge transfer. The performance and safety of Li-ion batteries are strongly impacted by temperature. Battery kinetics is sluggish at low temperature, while aging accelerates at high temperature and extreme temperature conditions can trigger thermal runaway. Enabling XFC requires detailed understanding of temperature effects on batteries and the development of weather-independent thermal management solutions.

The main concern of XFC at low temperatures is the risk of Li plating[78,79]. Kinetic processes affect Li plating, as ionic conduction in electrolyte and reactions at graphite surfaces all slow down substantially with decreasing temperature following the Arrhenius relation. Therefore, most of today's EVs do not support fast charging at low temperatures unless auxiliary pre-heating is enabled. For example, Nissan Leaf can be charged to 80% SoC in 30 minutes at room temperature, but requires >90 minutes at lower temperatures[80]. Simulation of the Li-deposition potential showed that a 9.5 Ah PHEV cell capable of charging at 4C without Li plating at 25 °C can only allow 1.5C charging at 10 °C and C/1.5 charging at 0 °C to avoid Li plating[79].

To enhance the cold-climate charging ability, a common practice is to pre-heat the batteries. For XFC, external heaters may not be sufficient due to the relatively slow thermal conduction from cell surface to centre. Therefore, battery internal heating for rapid, uniform warming has been proposed[79,81]. For example, pre-heating a 9.5 Ah pouch cell from −50 °C to room temperature within 1 minute was demonstrated by embedding a multilayer nickel foil as both the heater and the temperature sensor into the battery, such that the battery can reach 80% SoC within 15 minutes in a −50 °C environment, with good 3.5C charging cycling performance at 0 °C (ref. [79]). Alternative approaches have focused on improving battery components (electrodes, electrolytes and additives) to be suitable over a wider temperature range, as summarized in a recent review[82]. Nonetheless, many of the methods are only beneficial at either low or high temperatures.

High temperatures, which accelerate side reactions and electrode degradations, also present significant challenges for XFC[83]. Nissan Leaf had encountered problems with battery capacity fading in the hot Arizona climate. Importantly, the excessive heat generation from joule heating and electrode reaction during XFC can further elevate the temperature[5]. Figure 4a shows that the surface temperature of pouch cells increases pronouncedly with C-rate under natural convection conditions[84]. Thus, if the thermal management system is not designed properly, battery temperature during fast charging could reach abuse conditions and trigger thermal runaway (uncontrollable release of heat due to exothermic reactions), leading to catastrophic safety hazards[85,86]. A simulation study suggested that with poor thermal management, the average temperature of a pouch cell can reach 350 °C in 750 s with 350 kW XFC[5], which is far beyond the onset of thermal runaway and the melting temperature of the commonly used separators[87]. Apparently, enabling XFC will require research efforts ranging from understanding of heat generation and the development of advanced temperature-sensing techniques, to designing cell- to pack-level thermal management systems. A few specific issues are briefly discussed here with possible mitigation measures proposed.

One issue is that the high volumetric heat generation rate during XFC can lead to spatially non-uniform temperature distribution inside a battery, besides the overall increase in temperature (Fig. 4b). Temperature heterogeneity can arise from factors including anisotropic heat-spreading resistance within the cell, a non-uniform cooling environment as in the cooling design of some of today's EVs, contact resistance at tabs and manufacturing defects, all of which exacerbate as the C-rate increases[82]. More importantly, electrochemical reactions are positively affected by temperature following the Arrhenius law, such that local high temperature increases local current, which in turn releases more heat that raises the temperature (Fig. 4c). This electrochemical–thermal positive feedback

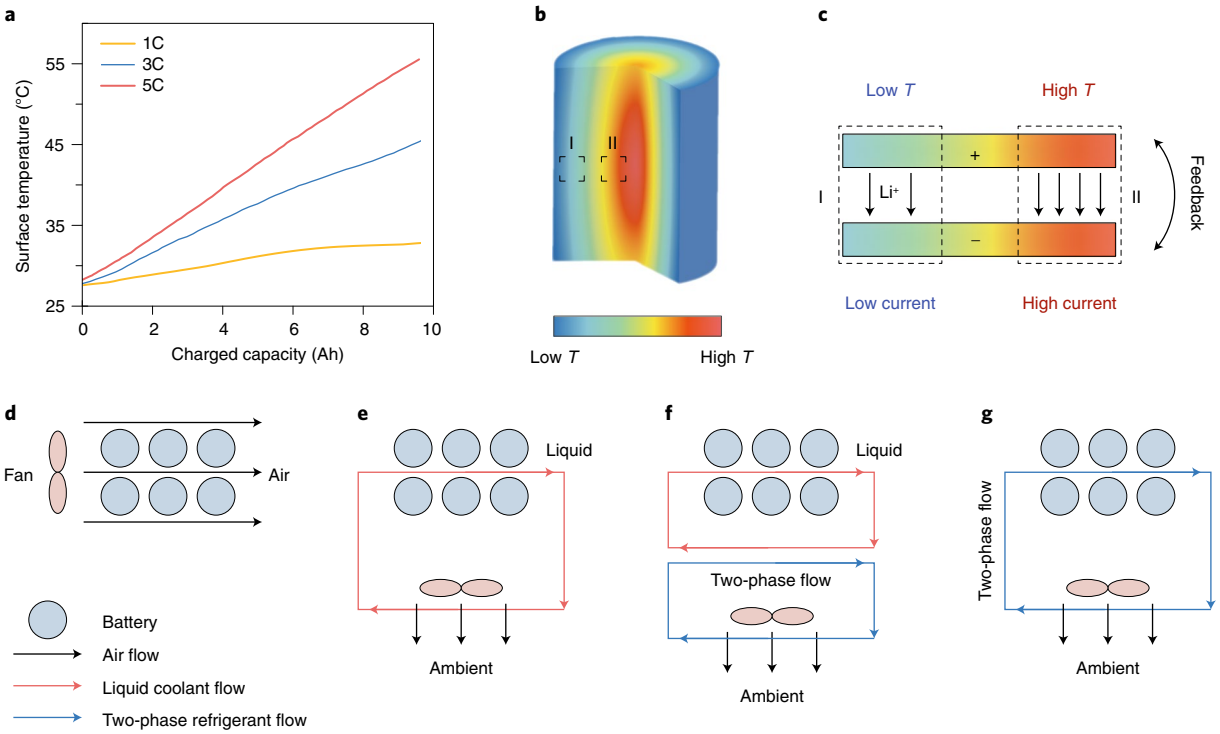

Fig. 4 | Battery thermal considerations during fast charging. a, External surface temperature of a laminated stack plate pouch cell at different charging rates under natural convection conditions[84]. **b**, Schematic of elevated, non-uniform temperature (*T*) inside a battery during fast charging due to high current and heat accumulation. **c**, Positive feedback between temperature and current. Local high temperature promotes transport and reaction and therefore increases local current, which in turn releases more heat that further elevates temperature. **d**–**g**, Thermal management systems of EV batteries using air cooling (**d**), liquid cooling to transport heat from batteries to the ambient air (**e**), liquid cooling interfaced with a refrigerant cycle to further lower the liquid coolant temperature (**f**) and two-phase refrigerant cooling with greatly enhanced heat transfer coefficient (**g**). Detailed components, including pumps, compressors and heat exchangers, are not shown. Panel **a** adapted from ref. [84], Elsevier.

may cause spatial inhomogeneity of the SoC. To comprehensively analyse this effect, advanced non-invasive sensing techniques that can probe battery internal temperature with high spatial resolution need to be developed, which can be further compared with local electrochemical characterizations. Such sensing capabilities may also be employed as part of the EV battery management system, and potentially aid the early detection of thermal runaway. Temperature non-uniformity can be suppressed by improving the thermal conductivity of battery components such as the separator[88], utilizing the heat path along the high-thermal-conductivity metal current collectors[89], and ensuring uniform thermal contact between the batteries and the active thermal management system.

Another issue is the potential trade-off between energy density and thermal performance of batteries. Common design strategies to meet the high-energy-density goal alongside XFC, including increasing the electrode thickness, light-weighting the current collector and decreasing electrochemically inactive materials, could raise the cell resistance causing increased joule heating (normally up to 50% of total heat generation)[90]. These designs may also reduce the effective thermal conductivity, hindering efficient heat extraction. Therefore, when designing new high-energy-density batteries with XFC capability, it is essential to also evaluate and balance their impact on the batteries' thermal performance.

With increased charging rates, more aggressive thermal management is needed. Air cooling by forced convection (Fig. 4d) in some of today's EVs will not meet the requirement for XFC due to the low heat transfer coefficient (up to ~100 W m^{-1} K^{-1}). Liquid cooling (typically with ethylene glycol as the coolant) that circulates to transport heat from battery packs to ambient air through a radiator (Fig. 4e) may not be sufficient either, especially in hot climates. Some EVs utilize a separate vapour compression refrigerant (VCR) system (two-phase cooling) to extract heat from the coolant loop (Fig. 4f)[91]. This design is advantageous because the VCR system can lower the coolant temperature below ambient. However, higher pumping power consumption may be expected to increase the coolant flow rate to enhance the convective heat transfer coefficient. Moving forward, direct integration of a scaled-up two-phase cooling system (such as a VCR cycle) with the battery pack (Fig. 4g) will greatly enhance the heat-removing ability and heat-transfer efficiency. Such a system requires complex design, potentially with a higher cost, but is worth investigating for its cooling potential.

Temperature control may also be implemented at XFC stations where a microclimate zone is created surrounding the batteries through localized air-conditioning or other means, making XFC independent of the actual weather[5]. Owing to the drastically different battery heat-generation rates under XFC and normal charge/discharge mode, adaptive battery thermal management system to satisfy the varying cooling load through advanced passive or active control[92] and machine learning will be desired.

Characterization tools for fundamental insight

Advanced characterization tools, especially with high spatial and/or temporal resolution, can critically inform materials design and may reveal new failure modes during XFC. As the dynamic processes within batteries span multiple length and time scales, a combination of different techniques is often needed. Herein, we highlight X-ray-based techniques and cryo-EM, which are deemed powerful in answering some of the most pressing fundamental questions during

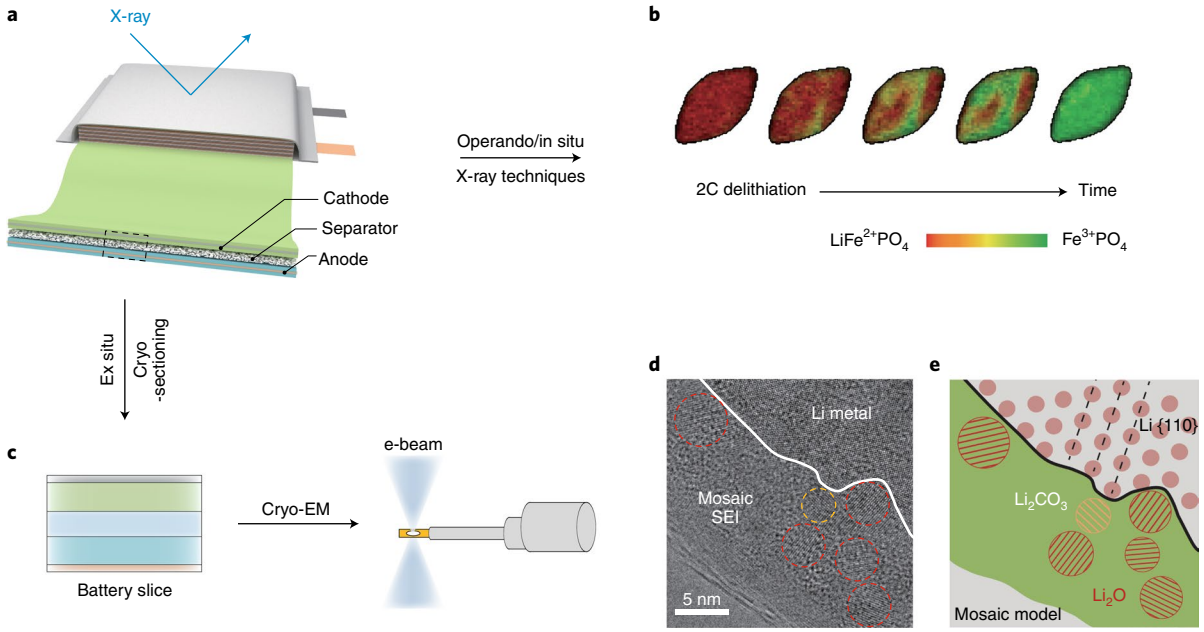

Fig. 5 | Advanced characterization techniques to fundamentally understand the battery failure mechanisms during fast charging. a, Operando and in situ X-ray techniques can be utilized to study the structural and compositional evolution of prototypical cells over repeated XFC cycling. **b**, An example of using operando scanning transmission X-ray microscopy to characterize the electrode heterogeneity during charging. Li composition across a single LFP particle during delithiation has been mapped[99]. **c**, Slices of cycled full cells can be obtained via cryo-sectioning techniques such as cryo-FIB and cryo-ultramicrotomy for cryo-EM studies. **d**,**e**, An example of a cryo-EM study on the microstructure of the SEI. **d**, Atomic-resolution image of the SEI on Li metal surface. **e**, The corresponding schematic of the observed mosaic-type SEI[50]. Panels reproduced from: **b**, ref. [99], AAAS; **d**,**e**, ref. [50], AAAS.

XFC. Interested readers are referred to recent reviews for exhaustive summaries on the state-of-the-art characterization techniques for batteries[93,94].

The good penetration depth and high brilliance of synchrotron radiation render X-ray-based techniques attractive for non-destructive characterizations of batteries during operation, particularly at the microscale (electrode and particle levels). Though most of the reported in situ or operando X-ray studies on batteries have focused on relatively slow kinetics and short cycling history (a few cycles)[93], with the advancement of fast data collection techniques and cell design, vast opportunities exist for XFC research to interrogate the structural and compositional evolution of prototypical full cells over repeated cycling (Fig. 5a).

The effects of high-rate charging on cathodes are rarely discussed in the literature, which necessitates more systematic studies. A few reports show that the cracking of secondary particles, caused by anisotropic structural changes and SoC heterogeneities, exacerbates at high currents[95]. In this respect, X-ray computed tomography can be used to enable high-resolution visualization of such morphological degradation processes[96]. At the crystal structure level, the presence of high overpotential during XFC may drive the electrochemical reaction away from thermodynamic equilibrium. For example, using operando time-resolved X-ray diffraction (XRD) with ultrafast spectrum acquisition (4 s), Liu et al. observed that the delithiation of $LiFePO_4$ (LFP) at high rates (>5C) proceeded via a continuous structural change rather than a distinct two-phase reaction[97]. With the same technique, Zhou et al. observed the formation of an intermediate phase in NMC111 when charged at high C-rates (>10C), which was hypothesized to serve as a buffer to local stress[98]. While XRD provides structural information during cycling, spectroscopy techniques (for example, X-ray absorption spectroscopy) can identify the kinetic contributions from different metal centres to inform cathode design with better rate performance[94]. Besides understanding the ensemble behaviour, special attention needs to be given to the heterogeneity within and between particles across the three dimensions of the electrode during XFC. Non-uniform charging locally concentrates the current, which can be directly correlated to other electrochemical, mechanical and thermal degradations. For example, employing operando scanning transmission X-ray microscopy and a microfluidic electrochemical cell, Lim et al. investigated the SoC distribution within individual LFP particles during cycling by tracking the Fe oxidation state with a 50 nm probe. Delithiation was found to be substantially less uniform than lithiation, and, surprisingly, compositionally non-uniform solid solution domains were observed for all the C-rates studied (up to 2C; Fig. 5b)[99].

For anodes, techniques such as X-ray computed tomography and spatially resolved XRD[100] can be useful when probing local parasitic Li depositions in pouch cells. Questions that might be answered include how and where does metallic Li plate during fast charging, what is the correlation between electrode structure and Li plating, how does the plated Li evolve during repeated cycling, and so on.

In addition to X-ray-based studies during battery operation, ex situ high-resolution imaging can provide critical complementary information at the nano- and atomic scales. Cryo-EM has very recently been adapted to study reactive and sensitive battery materials (Fig. 5c)[50–52]. In the first demonstration, the atomic column of metallic Li and the nanostructure of the SEI were observed (Fig. 5d,e)[50]. Later, the Kourkoutis group coupled cryogenic scanning transmission electron microscopy with cryogenic focused ion beam (cryo-FIB) to image the solid/liquid interface within batteries[52]. Rich chemical information can also be obtained when combining cryo-imaging with techniques such as electron energy loss spectroscopy and energy dispersive spectroscopy. Such initial success of cryo-EM showcases the exciting opportunities for scientific discovery within the battery community.

In the future, cycled full cells and large electrode particles can be thinned with cryogenic sectioning techniques, such as cryo-FIB and cryo-ultramicrotomy, to make them suitable for cryo-EM imaging. Several important directions can be pursued for XFC research. First, the SEI nanostructure on graphite is dependent on factors such as electrolyte composition and formation conditions, and different SEIs can in turn afford different charge-transfer kinetics. Therefore, elucidating the correlation between these terms is extremely valuable to realize more informed battery development. Second, taking advantage of the high resolution of cyro-EM, the initial nucleation of metallic Li on graphite can be captured, which is difficult to resolve with other techniques. Moreover, the intermediate phases of cathodes during cycling may have very short lifetimes, making them elusive to ex situ studies[94,99]. However, by freezing the battery during its operation, it is possible to quench these metastable states and observe them with cryo-EM, due to significantly reduced relaxation kinetics at cryogenic temperature. Last but not the least, by obtaining slices of an entire battery, cross-talks between battery components can be studied (the effect of cathode dissolution on the anode and Li plating, and so on) to uncover degradation mechanisms.

Outlook

In light of the abovementioned developmental needs at the battery level towards fast charging, each individual component of today's Li-ion batteries needs to be optimized in future research. Important directions include, but are not confined to, enhancing the transport properties of electrolytes, shortening the ion-diffusion distance by electrode architectural design, reducing Li-plating propensity with more sophisticated charging protocols, incorporating sensing functionalities inside batteries, developing advanced thermal management systems capable of efficiently and uniformly extract heat from batteries, and so on. As a battery is a delicate system and improvement of one parameter might negatively impact other battery metrics, step changes in Li-ion battery technologies call for a holistic approach. Furthermore, special research attention is required to find economical means to translate many of the proof-of-concept battery designs to scalable productions. Importantly, the successful realization of XFC also hinges on in-depth understanding of the degradation mechanisms under fast-charging conditions at both materials and cell levels, such that advanced characterization tools need to be critically employed for fundamental studies. In the long term, we believe disruptive battery technologies such as novel battery chemistries and 3D battery architectures are to be pursued to ultimately enable fast charging and widespread EV adoption. Given that XFC is a complicated topic, in addition to the materials challenges and solutions presented in this Review, system-level concerns and solutions being pursued in the industry are also extremely important. We thus call for industry experts to share their knowledge in the scientific literature to bridge the gap between the two communities for concerted efforts towards the fast-charging goal.

Received: 6 December 2018; Accepted: 30 April 2019;
Published online: 03 June 2019

References

1. Karner, D., Garetson, T. & Francfort, J. *EV Charging Infrastructure Roadmap* (Idaho National Laboratory, 2016); https://inldigitallibrary.inl.gov/sites/sti/sti/7245706.pdf
2. Standard J1772: Electric Vehicle and Plug in Hybrid Electric Vehicle Conductive Charge Coupler (Society of Automotive Engineers, 2017).
3. Howell, D. et al. *Enabling Fast Charging: A Technology Gap Assessment* No. INL/EXT-17-41638 (US Department of Energy, 2017).
4. Ahmed, S. et al. Enabling fast charging — a battery technology gap assessment. *J. Power Sources* **367**, 250–262 (2017).
This work reviewed the developmental needs towards extreme fast charging at the battery cell and pack levels.
5. Keyser, M. et al. Enabling fast charging — battery thermal considerations. *J. Power Sources* **367**, 228–236 (2017).
This work reviewed thermal challenges with regards to extreme fast charging.
6. Meintz, A. et al. Enabling fast charging — vehicle considerations. *J. Power Sources* **367**, 216–227 (2017).
7. Burnham, A. et al. Enabling fast charging — infrastructure and economic considerations. *J. Power Sources* **367**, 237–249 (2017).
8. Goodenough, J. B. & Kim, Y. Challenges for rechargeable Li batteries. *Chem. Mater.* **22**, 587–603 (2009).
9. Nyman, A., Zavalis, T. G., Elger, R., Behm, M. & Lindbergh, G. Analysis of the polarization in a Li-ion battery cell by numerical simulations. *J. Electrochem. Soc.* **157**, A1236–A1246 (2010).
10. Doyle, M., Fuller, T. F. & Newman, J. The importance of the lithium ion transference number in lithium/polymer cells. *Electrochim. Acta* **39**, 2073–2081 (1994).
11. Gallagher, K. G. et al. Optimizing areal capacities through understanding the limitations of lithium-ion electrodes. *J. Electrochem. Soc.* **163**, A138–A149 (2016).
12. Logan, E. et al. A study of the physical properties of Li-ion battery electrolytes containing esters. *J. Electrochem. Soc.* **165**, A21–A30 (2018).
13. Smart, M., Ratnakumar, B., Chin, K. & Whitcanack, L. Lithium-ion electrolytes containing ester cosolvents for improved low temperature performance. *J. Electrochem. Soc.* **157**, A1361–A1374 (2010).
14. Smart, M., Ratnakumar, B. & Surampudi, S. Use of organic esters as cosolvents in electrolytes for lithium-ion batteries with improved low temperature performance. *J. Electrochem. Soc.* **149**, A361–A370 (2002).
15. Lagadec, M. F., Zahn, R. & Wood, V. Characterization and performance evaluation of lithium-ion battery separators. *Nat. Energy* **4**, 16–25 (2019).
16. Lee, H., Yanilmaz, M., Toprakci, O., Fu, K. & Zhang, X. A review of recent developments in membrane separators for rechargeable lithium-ion batteries. *Energy Environ. Sci.* **7**, 3857–3886 (2014).
17. Diederichsen, K. M., McShane, E. J. & McCloskey, B. D. Promising routes to a high Li^+ transference number electrolyte for lithium ion batteries. *ACS Energy Lett.* **2**, 2563–2575 (2017).
18. Xu, K. Nonaqueous liquid electrolytes for lithium-based rechargeable batteries. *Chem. Rev.* **104**, 4303–4418 (2004).
19. Videa, M., Xu, W., Geil, B., Marzke, R. & Angell, C. A. High Li^+ self-diffusivity and transport number in novel electrolyte solutions. *J. Electrochem. Soc.* **148**, A1352–A1356 (2001).
20. Popovic, J. et al. High lithium transference number electrolytes containing tetratriflylpropene's lithium salt. *J. Phys. Chem. Lett.* **9**, 5116–5120 (2018).
21. Buss, H. G., Chan, S. Y., Lynd, N. A. & McCloskey, B. D. Nonaqueous polyelectrolyte solutions as liquid electrolytes with high lithium ion transference number and conductivity. *ACS Energy Lett.* **2**, 481–487 (2017).
22. Schaefer, J. L., Yanga, D. A. & Archer, L. A. High lithium transference number electrolytes via creation of 3-dimensional, charged, nanoporous networks from dense functionalized nanoparticle composites. *Chem. Mater.* **25**, 834–839 (2013).
23. Suo, L., Hu, Y.-S., Li, H., Armand, M. & Chen, L. A new class of solvent-in-salt electrolyte for high-energy rechargeable metallic lithium batteries. *Nat. Commun.* **4**, 1481 (2013).
24. Varzi, A., Raccichini, R., Passerini, S. & Scrosati, B. Challenges and prospects of the role of solid electrolytes in the revitalization of lithium metal batteries. *J. Mater. Chem. A* **4**, 17251–17259 (2016).
25. Kato, Y. et al. High-power all-solid-state batteries using sulfide superionic conductors. *Nat. Energy* **1**, 16030 (2016).
26. Kerman, K., Luntz, A., Viswanathan, V., Chiang, Y.-M. & Chen, Z. Practical challenges hindering the development of solid state Li ion batteries. *J. Electrochem. Soc.* **164**, A1731–A1744 (2017).
27. Hitz, G. T. et al. High-rate lithium cycling in a scalable trilayer Li-garnet-electrolyte architecture. *Mater. Today* **22**, 50–57 (2019).
28. Zhang, H. et al. Single lithium-ion conducting solid polymer electrolytes: advances and perspectives. *Chem. Soc. Rev.* **46**, 797–815 (2017).
29. Aetukuri, N. B. et al. Flexible ion-conducting composite membranes for lithium batteries. *Adv. Energy Mater.* **5**, 1500265 (2015).
30. Porcarelli, L. et al. Single-ion conducting polymer electrolytes for lithium metal polymer batteries that operate at ambient temperature. *ACS Energy Lett.* **1**, 678–682 (2016).
31. Oh, H. et al. Poly(arylene ether)-based single-ion conductors for lithium-ion batteries. *Chem. Mater.* **28**, 188–196 (2015).
32. Harris, S. J. & Lu, P. Effects of inhomogeneities — nanoscale to mesoscale — on the durability of Li-ion batteries. *J. Phys. Chem. C.* **117**, 6481–6492 (2013).
33. Thorat, I. V. et al. Quantifying tortuosity in porous Li-ion battery materials. *J. Power Sources* **188**, 592–600 (2009).
34. Billaud, J., Bouville, F., Magrini, T., Villevieille, C. & Studart, A. R. Magnetically aligned graphite electrodes for high-rate performance Li-ion batteries. *Nat. Energy* **1**, 16097 (2016).

35. Bae, C. J., Erdonmez, C. K., Halloran, J. W. & Chiang, Y. M. Design of battery electrodes with dual-scale porosity to minimize tortuosity and maximize performance. *Adv. Mater.* **25**, 1254–1258 (2013).
36. Behr, S., Amin, R., Chiang, Y. & Tomsia, A. Highly-structured, additive-free lithium-ion cathodes by freeze-casting technology. *Ceram. Forum Int.* **92**, 39–43 (2015).
37. Sander, J., Erb, R. M., Li, L., Gurijala, A. & Chiang, Y.-M. High-performance battery electrodes via magnetic templating. *Nat. Energy* **1**, 16099 (2016).
38. Long, J. W., Dunn, B., Rolison, D. R. & White, H. S. Three-dimensional battery architectures. *Chem. Rev.* **104**, 4463–4492 (2004).
39. Pikul, J. H., Zhang, H. G., Cho, J., Braun, P. V. & King, W. P. High-power lithium ion microbatteries from interdigitated three-dimensional bicontinuous nanoporous electrodes. *Nat. Commun.* **4**, 1732 (2013).
40. Li, G. et al. Stable metal battery anodes enabled by polyethylenimine sponge hosts by way of electrokinetic effects. *Nat. Energy* **3**, 1076–1083 (2018).
41. Chu, H.-C. & Tuan, H.-Y. High-performance lithium-ion batteries with 1.5 μm thin copper nanowire foil as a current collector. *J. Power Sources* **346**, 40–48 (2017).
42. Jow, T. R., Delp, S. A., Allen, J. L., Jones, J.-P. & Smart, M. C. Factors limiting Li^+ charge transfer kinetics in Li-ion batteries. *J. Electrochem. Soc.* **165**, A361–A367 (2018).
43. Abe, T., Sagane, F., Ohtsuka, M., Iriyama, Y. & Ogumi, Z. Lithium-ion transfer at the interface between lithium-ion conductive ceramic electrolyte and liquid electrolyte — a key to enhancing the rate capability of lithium-ion batteries. *J. Electrochem. Soc.* **152**, A2151–A2154 (2005).
44. Xu, K., von Cresce, A. & Lee, U. Differentiating contributions to "ion transfer" barrier from interphasial resistance and Li^+ desolvation at electrolyte/graphite interface. *Langmuir* **26**, 11538–11543 (2010).
45. Peled, E. & Menkin, S. SEI: past, present and future. *J. Electrochem. Soc.* **164**, A1703–A1719 (2017).
46. Liu, Y. et al. Solubility-mediated sustained release enabling nitrate additive in carbonate electrolytes for stable lithium metal anode. *Nat. Commun.* **9**, 3656 (2018).
47. Komaba, S., Ozeki, T. & Okushi, K. Functional interface of polymer modified graphite anode. *J. Power Sources* **189**, 197–203 (2009).
48. Ming, J. et al. New insights on graphite anode stability in rechargeable batteries: Li ion coordination structures prevail over solid electrolyte interphases. *ACS Energy Lett.* **3**, 335–340 (2018).
49. Xu, K. Electrolytes and interphases in Li-ion batteries and beyond. *Chem. Rev.* **114**, 11503–11618 (2014).
50. Li, Y. et al. Atomic structure of sensitive battery materials and interfaces revealed by cryo-electron microscopy. *Science* **358**, 506–510 (2017).
This work demonstrated the use of cryo-electron microscopy for characterizing battery materials.
51. Wang, X. et al. New insights on the structure of electrochemically deposited lithium metal and its solid electrolyte interphases via cryogenic TEM. *Nano Lett.* **17**, 7606–7612 (2017).
52. Zachman, M. J., Tu, Z., Choudhury, S., Archer, L. A. & Kourkoutis, L. F. Cryo-STEM mapping of solid-liquid interfaces and dendrites in lithium-metal batteries. *Nature* **560**, 345–349 (2018).
53. Li, F. S., Wu, Y. S., Chou, J., Winter, M. & Wu, N. L. A mechanically robust and highly ion-conductive polymer-blend coating for high-power and long-life lithium-ion battery anodes. *Adv. Mater.* **27**, 130–137 (2015).
54. Wang, C., Zhao, H., Wang, J., Wang, J. & Lv, P. Electrochemical performance of modified artificial graphite as anode material for lithium ion batteries. *Ionics* **19**, 221–226 (2013).
55. Persson, K. et al. Lithium diffusion in graphitic carbon. *J. Phys. Chem. Lett.* **1**, 1176–1180 (2010).
56. Cheng, Q., Yuge, R., Nakahara, K., Tamura, N. & Miyamoto, S. KOH etched graphite for fast chargeable lithium-ion batteries. *J. Power Sources* **284**, 258–263 (2015).
57. Kim, N., Chae, S., Ma, J., Ko, M. & Cho, J. Fast-charging high-energy lithium-ion batteries via implantation of amorphous silicon nanolayer in edge-plane activated graphite anodes. *Nat. Commun.* **8**, 812 (2017).
This work demonstrated a fast-charging hybrid anode of an amorphous silicon nanolayer and edge-site-activated graphite.
58. Lin, D., Liu, Y. & Cui, Y. Reviving the lithium metal anode for high-energy batteries. *Nat. Nanotechnol.* **12**, 194–206 (2017).
59. Yan, K. et al. Selective deposition and stable encapsulation of lithium through heterogeneous seeded growth. *Nat. Energy* **1**, 16010 (2016).
60. Sun, Y. et al. Graphite-encapsulated Li-metal hybrid anodes for high-capacity Li batteries. *Chem* **1**, 287–297 (2016).
61. Burns, J., Stevens, D. & Dahn, J. In-situ detection of lithium plating using high precision coulometry. *J. Electrochem. Soc.* **162**, A959–A964 (2015).
62. Downie, L. et al. In situ detection of lithium plating on graphite electrodes by electrochemical calorimetry. *J. Electrochem. Soc.* **160**, A588–A594 (2013).
63. Wu, H., Zhuo, D., Kong, D. & Cui, Y. Improving battery safety by early detection of internal shorting with a bifunctional separator. *Nat. Commun.* **5**, 5193 (2014).
64. Liu, K. et al. Electrospun core–shell microfiber separator with thermal-triggered flame-retardant properties for lithium-ion batteries. *Sci. Adv.* **3**, e1601978 (2017).
65. Takami, N., Satoh, A., Hara, M. & Ohsaki, T. Structural and kinetic characterization of lithium intercalation into carbon anodes for secondary lithium batteries. *J. Electrochem. Soc.* **142**, 371–379 (1995).
66. Severson, K. A. et al. Data-driven prediction of battery cycle life before capacity degradation. *Nat. Energy* **4**, 383–391 (2019).
This work utlized machine learning to predict battery lives based on data collected from the early stages of battery cycling.
67. Nitta, N., Wu, F., Lee, J. T. & Yushin, G. Li-ion battery materials: present and future. *Mater. Today* **18**, 252–264 (2015).
68. Jung, H.-G., Jang, M. W., Hassoun, J., Sun, Y.-K. & Scrosati, B. A high-rate long-life $Li_4Ti_5O_{12}$/Li[$Ni_{0.45}Co_{0.1}Mn_{1.45}$]$O_4$ lithium-ion battery. *Nat. Commun.* **2**, 516 (2011).
69. Han, J.-T., Huang, Y.-H. & Goodenough, J. B. New anode framework for rechargeable lithium batteries. *Chem. Mater.* **23**, 2027–2029 (2011).
70. Takami, N. et al. High-energy, fast-charging, long-life lithium-ion batteries using $TiNb_2O_7$ anodes for automotive applications. *J. Power Sources* **396**, 429–436 (2018).
71. Son, I. H. et al. Silicon carbide-free graphene growth on silicon for lithium-ion battery with high volumetric energy density. *Nat. Commun.* **6**, 7393 (2015).
72. Sun, J. et al. A phosphorene–graphene hybrid material as a high-capacity anode for sodium-ion batteries. *Nat. Nanotechnol.* **10**, 980–985 (2015).
73. Li, W. et al. Amorphous red phosphorus embedded in highly ordered mesoporous carbon with superior lithium and sodium storage capacity. *Nano Lett.* **16**, 1546–1553 (2016).
74. Tang, Y., Zhang, Y., Li, W., Ma, B. & Chen, X. Rational material design for ultrafast rechargeable lithium-ion batteries. *Chem. Soc. Rev.* **44**, 5926–5940 (2015).
75. Lin, D. et al. Layered reduced graphene oxide with nanoscale interlayer gaps as a stable host for lithium metal anodes. *Nat. Nanotechnol.* **11**, 626–632 (2016).
76. Zheng, J. et al. Electrolyte additive enabled fast charging and stable cycling lithium metal batteries. *Nat. Energy* **2**, 17012 (2017).
77. Mao, C., Ruther, R. E., Li, J., Du, Z. & Belharouak, I. Identifying the limiting electrode in lithium ion batteries for extreme fast charging. *Electrochem. Commun.* **97**, 37–41 (2018).
78. Li, Z., Huang, J., Liaw, B. Y., Metzler, V. & Zhang, J. A review of lithium deposition in lithium-ion and lithium metal secondary batteries. *J. Power Sources* **254**, 168–182 (2014).
79. Yang, X.-G., Zhang, G., Ge, S. & Wang, C.-Y. Fast charging of lithium-ion batteries at all temperatures. *Proc. Natl Acad. Sci. USA* **115**, 7266–7271 (2018).
This work demonstrated 15-minute fast charging of Li-ion batteries in cold-temperature environments by preheating the battery with internal heaters.
80. *Nissan Leaf Owner's Manual* (Nissan Motor, 2017); https://cdn.dealereprocess.net/cdn/servicemanuals/nissan/2017-leaf.pdf
81. Wang, C.-Y. et al. Lithium-ion battery structure that self-heats at low temperatures. *Nature* **529**, 515–518 (2016).
82. Rodrigues, M.-T. F. et al. A materials perspective on Li-ion batteries at extreme temperatures. *Nat. Energy* **2**, 17108 (2017).
83. Leng, F., Tan, C. M. & Pecht, M. Effect of temperature on the aging rate of Li ion battery operating above room temperature. *Sci. Rep.* **5**, 12967 (2015).
84. Ye, Y., Saw, L. H., Shi, Y., Somasundaram, K. & Tay, A. A. O. Effect of thermal contact resistances on fast charging of large format lithium ion batteries. *Electrochim. Acta* **134**, 327–337 (2014).
85. Bandhauer, T. M., Garimella, S. & Fuller, T. F. A critical review of thermal issues in lithium-ion batteries. *J. Electrochem. Soc.* **158**, R1–R25 (2011).
86. Liu, K., Liu, Y., Lin, D., Pei, A. & Cui, Y. Materials for lithium-ion battery safety. *Sci. Adv.* **4**, eaas9820 (2018).
87. W. Golubkov, A. et al. Thermal-runaway experiments on consumer Li-ion batteries with metal-oxide and olivin-type cathodes. *RSC Adv.* **4**, 3633–3642 (2014).
88. Yang, Y., Huang, X., Cao, Z. & Chen, G. Thermally conductive separator with hierarchical nano/microstructures for improving thermal management of batteries. *Nano Energy* **22**, 301–309 (2016).
89. Hunt, I. A., Zhao, Y., Patel, Y. & Offer, G. J. Surface cooling causes accelerated degradation compared to tab cooling for lithium-ion pouch cells. *J. Electrochem. Soc.* **163**, A1846–A1852 (2016).
90. Srinivasan, V. & Wang, C. Y. Analysis of electrochemical and thermal behavior of Li-ion cells. *J. Electrochem. Soc.* **150**, A98–A106 (2003).
91. Tennessen, P. T., Weintraub, J. C. & Hermann, W. A. Extruded and ribbed thermal interface for use with a battery cooling system. US patent US8758924B2 (2014).
92. Hao, M., Li, J., Park, S., Moura, S. & Dames, C. Efficient thermal management of Li-ion batteries with a passive interfacial thermal regulator based on a shape memory alloy. *Nat. Energy* **3**, 899–906 (2018).

93. Lu, J., Wu, T. & Amine, K. State-of-the–art characterization techniques for advanced lithium-ion batteries. *Nat. Energy* **2**, 17011 (2017).
94. Hu, E., Wang, X., Yu, X. & Yang, X.-Q. Probing the complexities of structural changes in layered oxide cathode materials for Li-ion batteries during fast charge-discharge cycling and heating. *Acc. Chem. Res.* **51**, 290–298 (2018).
This work reviewed major characterization techniques at multilength scales for monitoring the structural evolution and kinetic characteristics of layered transition metal oxides during fast charge/discharge.
95. Xia, S. et al. Chemomechanical interplay of layered cathode materials undergoing fast charging in lithium batteries. *Nano Energy* **53**, 753–762 (2018).
96. Wood, V. X-ray tomography for battery research and development. *Nat. Rev. Mater.* **3**, 293–295 (2018).
97. Liu, H. et al. Capturing metastable structures during high-rate cycling of $LiFePO_4$ nanoparticle electrodes. *Science* **344**, 1252817 (2014).
98. Zhou, Y. N. et al. High-rate charging induced intermediate phases and structural changes of layer-structured cathode for lithium-ion batteries. *Adv. Energy Mater.* **6**, 1600597 (2016).
99. Lim, J. et al. Origin and hysteresis of lithium compositional spatiodynamics within battery primary particles. *Science* **353**, 566–571 (2016).
100. Oddershede, J. et al. Determining grain resolved stresses in polycrystalline materials using three-dimensional X-ray diffraction. *J. Appl. Crystallogr.* **43**, 539–549 (2010).

Acknowledgements

This work was supported by the Assistant Secretary for Energy Efficiency and Renewable Energy, Office of Vehicle Technologies of the US Department of Energy under the eXtreme Fast Charge Cell Evaluation of Li-ion batteries (XCEL) programme.

Competing interests

The authors declare no competing interests.

Additional information

Reprints and permissions information is available at www.nature.com/reprints.

Correspondence should be addressed to Y.C.

Publisher's note: Springer Nature remains neutral with regard to jurisdictional claims in published maps and institutional affiliations.